Mar Biol (2008) 154:37–49
DOI 10.1007/s00227-007-0895-6

RESEARCH ARTICLE

Estimation of the attachment strength of the shingle sea urchin, *Colobocentrotus atratus*, and comparison with three sympatric echinoids

Romana Santos · Patrick Flammang

Received: 24 May 2007 / Accepted: 18 December 2007 / Published online: 23 January 2008

Abstract The peculiar limpet-like morphology of the genus *Colobocentrotus* is unique among the regular echinoids. This shape has been interpreted as an adaptation to life in areas of extreme wave exposure. In this study the attachment strength of *C. atratus* is compared with that of three sympatric species, *Echinometra mathaei*, *Heterocentrotus trigonarius* and *Stomopneustes variolaris*, which have more typical echinoid morphology and live in different microhabitats. For each species, the adhesion of individual sea urchins was measured as well as the tenacity of single tube foot and the mechanical properties of the tube foot stems. *Colobocentrotus* always presented the highest measured values, although not always significantly different from those of the other species. Of the mechanical properties of the stem measured, the stem extensibility was the only property that was significantly different among species. In general the stems of all the species studied became more extensible and more difficult to break with increasing strain rate, providing an adaptative advantage to the sea urchin when subjected to rapid loads such as waves. In terms of single tube foot tenacity, *C. atratus* tube feet attached with a tenacity (0.54 MPa) two times higher than the one of *E. mathaei*, *H. trigonarius* and *S. variolaris* (0.21–0.25 MPa). Individual sea urchins of the four species, however, attached with a similar strength (0.2–0.26 MPa). The calculation of safety factors showed that it is the very high number of adoral tube feet of *C. atratus* and not the overall shape of the animal that allows this species to withstand very high water velocities. However, *C. atratus* streamlined morphology may be a functional adaptation to reduce the impact of other hydrodynamic forces (such as wave impingement forces) or to cope with other selective environmental stresses (such as dessication), and thus to inhabit extremely exposed areas of the intertidal.

Introduction

Throughout the Indo West Pacific, the shingle sea urchin *Colobocentrotus atratus* occupies areas of extreme wave climate (Mortensen 1943; Ebert 1982; Conand et al. 2003). The morphology of the genus *Colobocentrotus* is unique among the regular echinoids, its aboral spines are extremely reduced forming a smooth pavement, and the adoral part of the test is surrounded by a basal skirt of flattened spines (Agassiz 1908; Mortensen 1943; Gallien 1987), giving this sea urchin a limpet-like shape. These two features have long attracted the attention of functional morphologists and have led many observers to conclude that *C. atratus* morphology is an adaptation to life in wave-swept environments (Mortensen 1943; Hyman 1955).

Gallien (1987) further explored the influence of extreme wave exposure on sea urchin morphology by comparing the intertidal wave forces experienced by *C. atratus* with those

Communicated by M. Wahl.

R. Santos · P. Flammang
Académie Universitaire Wallonie-Bruxelles,
Université de Mons-Hainaut, Laboratoire de Biologie marine,
Pentagone 2B, 6 Avenue du Champ de Mars,
7000 Mons, Belgium

R. Santos (✉)
Instituto de Tecnologia Química e Biológica,
Laboratório de Espectrometria de Massa,
Avenida da República (EAN), Apartado 127,
2781-901 Oeiras, Portugal
e-mail: romana_santos@yahoo.com;
Patrick.Flammang@umh.ac.be

experienced by *Echinometra mathaei*, a sympatric sea urchin with a more typical echinoid morphology and a different microhabitat (it bores round holes into limestone reef, in which it seeks refuge from predators and hydrodynamics). Drag on *C. atratus* was reported to be substantially lower than on *E. mathaei*, which combined with its higher attachment strength (ratio of attachment force to sea urchins adoral surface area), resulted in a significant decrease of the risk of dislodgment of *C. atratus* by wave-induced forces comparatively to *E. mathaei*. This author proposed that this difference in the risk of dislodgment could help to explain both the evolutionary reduction of aboral spines in *C. atratus* and the behavioral confinement of *E. mathaei* to crevices and cavities. Denny and Gaylord (1996) re-examined Gallien's conclusions by accounting not only for drag but also for other hydrodynamic forces (lift and acceleration) imposed on sea urchins in their natural environment. They reported that the reduction in drag afforded by the *C. atratus* test morphology was largely offset by an increase in lift. In contrast, the acceleration force on *C. atratus* was found to be only half that of *E. mathaei*. As a consequence, these authors proposed that the "streamlined" morphology of *C. atratus* was an adaptation to reduce the force imposed by water acceleration, thereby making it feasible for *C. atratus* to venture safely into the rapid accelerations of the surf zone.

Although much is known about the influence of sea urchins morphology in reducing hydrodynamic load, the attachment strength with which sea urchins resist these forces has only been considered in a few studies. To withstand hydrodynamic forces, sea urchins are able to adhere strongly but temporarily to the substratum by means of a multitude of independent adhesive organs, the tube feet. Each tube foot consists of an enlarged and flattened distal extremity, the disc, which makes contact with and attaches to the substratum, and a proximal extensible cylinder, the stem which connects the disc to the animal body. Therefore, echinoid ability to inhabit high-energy environments has been attributed to a higher degree of development of their tube feet (i.e., larger and stickier discs and thicker and stronger stems; Sharp and Gray 1962; Smith 1978), combined with a higher number of tube feet involved in attachment (Märkel and Titschack 1965).

The present study aims at comparing the adhesive capacities of *C. atratus* with those of three sympatric species, *E. mathaei*, *Heterocentrotus trigonarius* and *Stomopneustes variolaris*, which have a more typical echinoid morphology and live in different micro-habitats. The boring sea urchin, *E. mathaei*, has a test often oval in aboral view with sharp, rigid and short spines. This species typically inhabits sheltered areas of the coral reef but it can also be found in more exposed areas where it hides in crevices or burrows (Régis and Thomassin 1982; De Ridder 1986; Conand et al. 2003). The slate pencil sea urchin, *H. trigonarius*, has a massive test, elliptic in shape and is slightly aboral-orally flattened. The primary spines can have variable shape, from thin, sharp and trihedral to thick, cylindrical and flared in club. The secondary spines are sharp or truncated forming a dense pavement limited to the apical system. This species can be found from the intertidal to shallow subtidal areas. They prefer high-energy environments; especially, the outer reef front and the fore-reef slope being often found in hollows in the reef (Régis and Thomassin 1982; De Ridder 1986; Conand et al. 2003). Finally, the black sea urchin, *S. variolaris*, has a round test with long and sharp spines. They can be found from the intertidal to the immediately subtidal in high-energy rocky shores where they live in holes or crevices (Régis and Thomassin 1982; De Ridder 1986; Conand et al. 2003). For each species, the attachment strength of individual sea urchins was measured as well as the tenacity of single tube foot discs and the mechanical properties of tube foot stems.

Materials and methods

Study site and specimens collection

Sea urchins were collected during low tide at Cap La Houssaye located on the northwest coast of the Reunion Island in the Indian Ocean (21°0′0″S, 55°13′60″E). At this location, the shore is essentially basaltic and exposed to relatively strong waves. Four species of sea urchins (Fig. 1) co-occur in this area: three Echinoida, *Colobocentrotus atratus* (Linnaeus, 1758), *Heterocentrotus trigonarius* (Linnaeus, 1758), *Echinometra mathaei* (Blainville, 1825), and one Phymosomatoida, *Stomopneustes variolaris* (Lamark, 1816). Although the four populations overlapped, the one of *C. atratus* was found on relatively flat rocks in higher areas of the intertidal. The three other populations inhabited the lower intertidal, often immersed even at low tide. Individuals of *E. mathaei* were often found in holes or crevices while specimens of *H. trigonarius* and *S. variolaris* were present in the same area but rarely hid in cavities. After collection, the animals were kept in open-circuit aquaria at 25°C and 35‰ at the "Aquarium de la Réunion" (Saint Gilles les Bains).

Tube foot mechanical properties

The stem

Measurements were carried out according to the protocol described in Santos and Flammang (2005) except that the

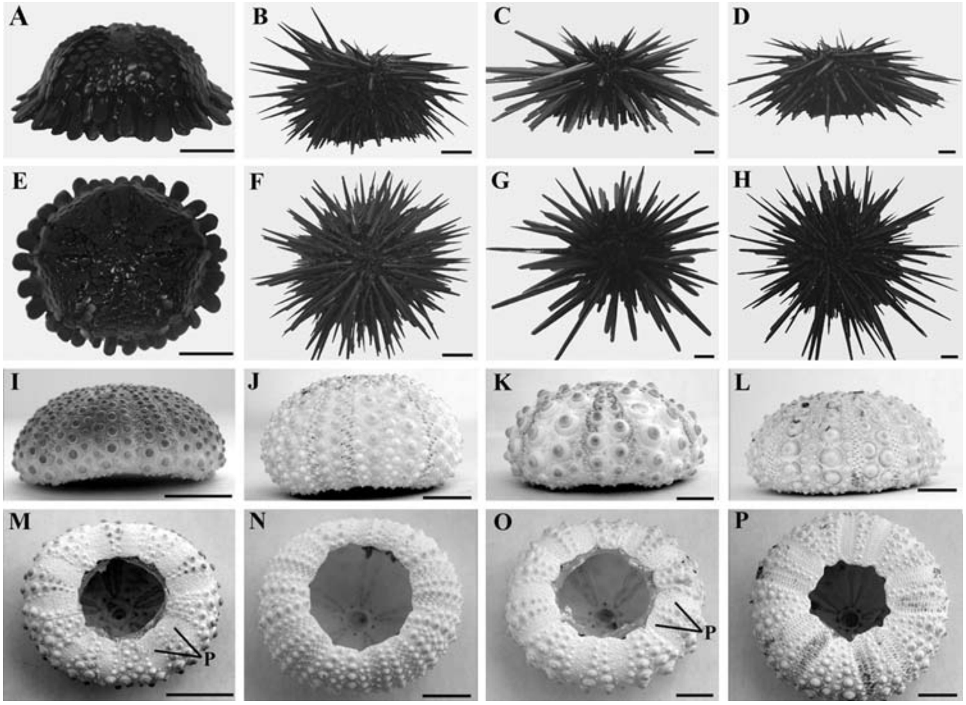

Fig. 1 Sea urchins used in this study: *Colobocentrotus atratus* (**a**, **e**, **i**, **m**), *Echinometra mathaei* (**b**, **f**, **j**, **n**), *Heterocentrotus trigonarius* (**c**, **g**, **k**, **o**) and *Stomopneutes variolaris* (**d**, **h**, **l**, **p**). Lateral (**a–d**) and aboral (**e–h**) view of whole sea urchins with spines, and lateral (**i–l**) and oral (**m–p**) view of tests without spines. Abbreviation: *P*, phyllode. *Scale bar* represents 10 mm

dynamometer (AFG 2.5 N; Mecmesin, Horsham, UK) was fitted on a manual stand. Sea urchins were placed upside down in containers filled with seawater and a small surgical clip was attached to one adoral tube foot, in the portion of the stem just under the disc. Then, the tube foot was pulled perpendicularly to the test of the sea urchin (i.e., in the direction of the natural extension), at relatively constant speed, until failure. Stem initial length together with the displacement registered by the manual stand (with a precision of 0.01 mm) at the moment of failure, were subsequently used to calculate stem final length. The extension rate was calculated as the ratio of stand displacement to time of extension. As for strain rate it was obtained by dividing the extension rate by the initial length of the tube foot.

During the mechanical test, data were continuously recorded as force–extension curves, which were then converted into stress–strain curves (see Santos and Flammang 2005). True values of strain and stress were used instead of nominal values because of the high extensions observed for the tube foot stems of the sea urchins (Shadwick 1992). True strain expresses the deformation of the tube foot in response to a certain force and, at the point at which the stem fails (at final length); it is a measure of the material's extensibility. Similarly, the maximum value of true stress (i.e., at breaking force) is an indicator of the tube foot tensile strength. Two other mechanical properties were calculated: the modulus, the highest slope of the stress–strain curve, and the breaking energy density, the energy needed to extend and break the tube foot. They are measures of the stem stiffness and toughness, respectively (see Vogel 2003, for review). These mechanical properties were measured on a total of 120 tube feet, i.e., ten tube feet from three individuals per species.

After the mechanical tests, ten non-tested tube feet were dissected from each specimen for the measurement of the mean cross-sectional areas of each tissue layer of the tube foot stem. These tube feet were fixed in Bouin's fluid for 24 h, subsequently dehydrated in a sequence of graded ethanol and embedded in paraffin wax. They were then cut transversely into 7 μm thick sections with a Microm HM 340 E microtome. The sections were mounted on clean glass slides and stained with Masson's Trichome. Measurements were made with a Leica Laborlux light microscope equipped with a graduated eyepiece on sections taken halfway between the base and the disc of the tube feet.

The disc

Adhesion force measurements of single tube feet were performed as described in Santos et al. (2005) and Santos and Flammang (2006). Experiments were carried out with sea urchins totally immersed in containers filled with seawater. Specimens were put upside-down (to induce tube foot attachment) and a 1 cm^2 piece of smooth polymethylmethacrylate (PMMA) connected to a dynamometer (AFG 10 N) by a surgical thread, was presented to the tube feet. When a single tube foot attached to the substratum, the dynamometer was manually moved upwards at approximately constant speed in order to apply a force normal to the disc. After tube foot detachment, the maximum force or critical detachment force was recorded. Then, the adhesive material (footprint) left on the substratum was stained with crystal violet and photographed to measure its surface area. After each measurement, the piece of substratum was either replaced by a new piece or carefully cleaned. The tenacity (expressed in N m^{-2} or Pascal) was then calculated by dividing the measured detachment force by the corresponding footprint surface area. For each species, measurements were carried out on about 30 tube feet, from at least four different sea urchins.

Individual sea urchin morphometry and attachment strength

Measurements of the attachment strength of individual sea urchins were performed according to Santos and Flammang (2007). Experiments were performed with sea urchins placed in small aquaria, the walls of which were covered internally by removable polystyrene (PS) plates. Animals were allowed 15 min to attach, after which they were clamped by the test with a loop of string connected to a dynamometer (AFG 250 N) and manually pulled upwards at approximate constant speed. After detachment, the maximum force required to dislodge the sea urchin was recorded as well as the angle of pull (0°, 45°, or 90° from the plane of the substratum), which varied according to the animal's position in the aquarium (on the side wall, in the corner or on the bottom, respectively). The PS plate(s) to which the animal was attached were removed from the aquarium, the broken tube feet were counted and discarded, and the plate(s) immediately stained as described for single tube feet. Digital photographs of the plate(s) were taken, each picture being calibrated with a piece of millimetric paper, and used to measure the total surface area of the footprints with the software Scion Image® 4.0.2 (Scion Corporation, Frederick, MD, USA). The total number of footprints was also counted, as well as the proportion of circular (tube foot attached with the entire disc) and irregular (tube foot attached with part of the disc) footprints. The tenacity of individual sea urchins (expressed in N m^{-2} or Pa) was calculated as the ratio of attachment force to footprint surface area. It was measured on 30 randomly chosen sea urchins of each species.

Immediately after each experiment, the animals were measured (test ambital diameter and height) and weighed (immersed weight). Moreover, three animals of each species (with sizes covering the whole ranges of sea urchin sizes for which attachment forces were measured) were cleaned to remove their tube feet and spines, in order to count the pores on the test and thus quantify the total number of adoral tube feet (Santos and Flammang 2007).

Safety factor

The safety factor was calculated as the ratio of sea urchin mean attachment force to mean maximum hydrodynamic force (see Santos and Flammang 2007). When this factor is ≤1, the animal is dislodged. The maximum hydrodynamic force exerted on sea urchins is due to both water velocity and acceleration (Denny 1988). However, Gaylord (2000) showed that forces imposed by acceleration are minimal and, therefore, they will not be considered in this study. Therefore, the maximum hydrodynamic force was obtained using the equation of Denny (1988):

$$F_{\text{environment}} = 1/2\,\rho\,u^2 \sqrt{\left[\left(C_{\text{drag}} S_{\text{profile}}\right)^2 + \left(C_{\text{lift}} S_{\text{planform}}\right)^2\right]}, \tag{1}$$

in which ρ, seawater density (1,024 kg m^{-3}); u, the water velocity in m s^{-1}; C_{drag}, the drag coefficient; $S_{\text{profile,}}$ the surface area of the sea urchin on which the drag force is exerted (in m^{-2}); $C_{\text{lift,}}$ the lift coefficient; $S_{\text{planform,}}$ the surface area of the urchin on which the lift force is exerted (in m^{-2}). Values for the drag and lift coefficients are those measured by Denny and Gaylord (1996) for the sea urchins *C. atratus* and *E. mathaei*; the latter being also used for the two other species considered in this study:

$$\textit{Colobocentrotus atratus}\ C_{\text{drag}} = 0.150 + 0.098\ \log\ Re \tag{2}$$

$$\textit{Colobocentrotus atratus}\ C_{\text{lift}} = -0.134 + 0.047\ \log\ Re \tag{3}$$

$$\textit{Echinometra mathaei}\ C_{\text{drag}} = 0.771 - 0.029\ \log\ Re \tag{4}$$

$$\textit{Echinometra mathaei}\ C_{\text{lift}} = -0.020 + 0.011\ \log\ Re \tag{5}$$

in which Re, the Reynolds number was calculated as:

$$Re = \rho\,u\,L/\mu, \tag{6}$$

where L is the sea urchin length (with spines, expressed in m) in the direction of the flow, and μ is the dynamic viscosity of seawater in kg m^{-1} s^{-1}. Mean projected profile (S_{profile}) and planform (S_{planform}) areas were calculated using three animals for each species whose sizes covered the range of sizes of the animals collected in the sampling area. Digital photographs of each individual were taken laterally (Fig. 1a–d) and from above (Fig. 1e–h), each picture being calibrated with millimetric paper. The surface areas (S_{profile} and S_{planform}, respectively) were then calculated with Scion Image®. The maximum attachment force was calculated as the product of tenacity by the total number of adoral tube feet and the surface area of a single tube foot disc.

Statistical analyses

All statistical tests were performed with the software Statistica® (Statsoft Inc., Tulsa, OK, USA). When necessary, data were log-transformed to achieve homoscedasticity and percentages were arcsine transformed to achieve normality. The results were analyzed in order to look for significant interspecific differences in terms of sea urchin morphometry and attachment strength, disc tenacity and stem mechanical properties, sea urchin individuals being always used as the replicate (i.e., when more than one measurement were made on one individual, the mean value for this individual was used in the tests). When analysis of variance (ANOVA) indicated significant effects ($P < 0.05$), the Tukey test was used for pair wise multiple comparisons. Simple linear regression analysis was also used to search for significant relationships between stem mechanical properties and strain rate; between the number of adoral tube feet and test diameter; and between sea urchin individual tenacity and test diameter, height and weight.

Results

Tube foot mechanical properties

Stem

Table 1 summarizes the results of the morphometric measurements on the tube foot stems for the four echinoid species. No interspecific differences were found in terms of stem diameter and initial length and in terms of stem wall thickness and cross-sectional area. Similarly to other echinoid tube feet (see Flammang 1996 for review), the stem wall of the four species studied consisted of four tissue layers: an inner myomesothelium surrounding the water-vascular lumen, a connective tissue layer, a nerve plexus, and an outer epidermis covered by a cuticle (Fig. 2a). Among these layers, only the connective tissue thickness and cross-sectional area varied significantly between species (Table 1). When cross-sectional areas of each tissue layer were expressed as percentages of the total stem wall cross-sectional area (Fig. 2b), the epidermis (including the basiepithelial nerve plexus) and the connective tissue were the dominant layers of the stem wall, representing about 37–48 and 30–42% of the stem cross-sectional area, respectively. As for the myomesothelium, it represented only about 20% of the stem cross-sectional area in the four species.

Table 1 Mean morphometric values (±SD, $n = 3$) for the adoral tube feet of *Colobocentrotus atratus, Echinometra mathei, Heterocentrotus trigonarius* and *Stomopneustes variolaris*

	Species				P_{ANOVA}
	Colobocentrotus atratus	*Echinometra mathaei*	*Heterocentrotus trigonarius*	*Stomopneutes variolaris*	
Tube foot measurement					
Stem diameter (mm)	0.464 ± 0.086^{a}	0.398 ± 0.074^{a}	0.508 ± 0.094^{a}	0.509 ± 0.074^{a}	0.370
Stem initial length (mm)	5.33 ± 1.40^{a}	5.20 ± 0.66^{a}	5.10 ± 0.53^{a}	6.57 ± 0.57^{a}	0.213
Tissue thicknesses					
Stem wall (mm)	0.130 ± 0.016^{a}	0.117 ± 0.022^{a}	0.159 ± 0.027^{a}	0.137 ± 0.016^{a}	0.182
Epidermis and nerve plexus (mm)	0.049 ± 0.007^{a}	0.042 ± 0.005^{a}	0.045 ± 0.011^{a}	0.051 ± 0.009^{a}	0.544
Connective tissue (mm)	0.044 ± 0.005^{a}	0.039 ± 0.011^{a}	0.066 ± 0.006^{b}	0.043 ± 0.005^{a}	0.018
Myomesothelium (mm)	0.037 ± 0.005^{a}	0.035 ± 0.007^{a}	0.049 ± 0.010^{a}	0.043 ± 0.005^{a}	0.179
Tissue cross-sectional areas					
Stem wall (mm^2)	0.128 ± 0.042^{a}	0.097 ± 0.040^{a}	0.175 ± 0.063^{a}	0.146 ± 0.037^{a}	0.284
Epidermis and nerve plexus (mm^2)	0.061 ± 0.019^{a}	0.045 ± 0.015^{a}	0.066 ± 0.028^{a}	0.069 ± 0.018^{a}	0.516
Connective tissue (mm^2)	0.041 ± 0.014^{a}	0.032 ± 0.017^{a}	0.072 ± 0.020^{b}	0.045 ± 0.010^{a}	0.008
Myomesothelium (mm^2)	0.026 ± 0.009^{a}	0.020 ± 0.008^{a}	0.037 ± 0.015^{a}	0.033 ± 0.007^{a}	0.272

Significant differences between means for a given parameter are indicated by letters in superscripts; means sharing at least one letter are not significantly different ($P_{\mathrm{Tukey}} \geq 0.05$)

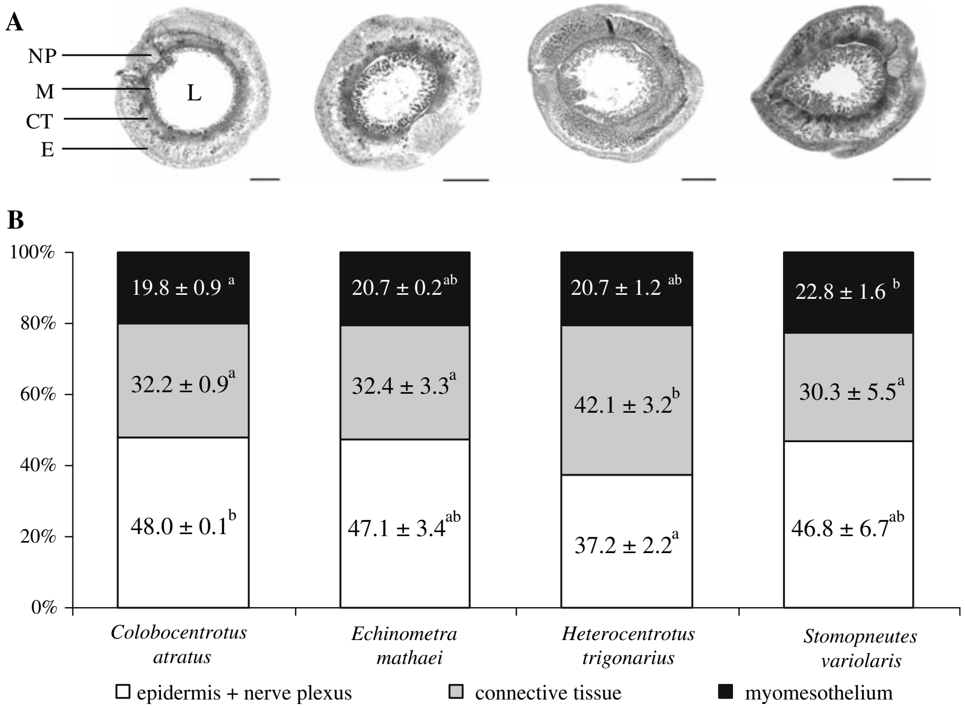

Fig. 2 *Colobocentrotus atratus*, *Echinometra mathaei, Heterocentrotus trigonarius* and *Stomopneustes variolaris*. Transverse sections through the stem of adoral tube feet showing stem wall tissue layers (**a**), and histogram showing the respective proportions (in percent) of each tissue layer in the total cross-sectional area of the stem (±SD, $n = 3$) (**b**). Significant interspecific differences between means for a given tissue are indicated by *letters* in superscript; means sharing at least one letter are not significantly different ($P > 0.05$, multiple comparison test of Tukey; percentages were arcsine transformed). *Bars* correspond to 100 µm. *CT*, Connective tissue; *E*, epidermis; *L*, lumen; *M*, mesothelium; *NP*, nerve plexus

In terms of stem mechanical properties, the tube feet of the four species produced typical J-shaped stress–strain curves having characteristically an initial region of low resistance to the applied force followed by a region presenting a sudden increase in stress until rupture. The connective tissue cross-sectional area was used for the calculations of the true stress because this tissue appears clearly as the layer bearing most of the load exerted on a tube foot (Santos and Flammang 2005). The mean values of the material properties measured for the tube foot stems of the four sea urchins species area presented in Table 2. For each property, the tube feet of *C. atratus* always showed the highest values. However, stem extensibility was the only property that was significantly different among species, being higher in *C. atratus* relatively to *S. variolaris* (Table 2).

The possible strain-rate dependence of the tube foot mechanical properties was also investigated. Tube foot extensibility was found to be strongly ($r^2 > 41\%$) and positively dependent on strain rate in the four species (Fig. 3a). As for strength, no significant dependence could be identified. Stiffness was significantly affected by strain rate only in *C. atratus* (Fig. 3b) but in a much smaller extent than extensibility. With the exception of *H. trigonarius*, all the species showed a positive relationship between tube foot toughness and strain rate, the latter explaining 17–28% of the variation in this parameter (Fig. 3c).

Disc

The force required to detach the tube feet of *C. atratus* (0.28N) was 2–4 times higher than the forces needed to detach tube feet from the three other species (0.06–0.12 N)

Table 2 Mean values (±SD, $n = 3$) of the material properties measured for tube foot stem of *Colobocentrotus atratus, Echinometra mathei, Heterocentrotus trigonarius* and *Stomopneustes variolaris*

	Species				P_{ANOVA}
	Colobocentrotus atratus	*Echinometra mathaei*	*Heterocentrotus trigonarius*	*Stomopneutes variolaris*	
Breaking force (N)	0.52 ± 0.11^{a}	0.31 ± 0.06^{a}	0.60 ± 0.25^{a}	0.47 ± 0.08^{a}	0.178
Extensibility	1.49 ± 0.15^{b}	1.21 ± 0.07^{ab}	1.35 ± 0.15^{ab}	1.17 ± 0.06^{a}	0.036
Strength (MPa)	59.94 ± 16.17^{a}	38.68 ± 8.60^{a}	32.21 ± 18.54^{a}	35.87 ± 5.70^{a}	0.123
Stiffness (MPa)	170.45 ± 45.97^{a}	102.98 ± 25.67^{a}	88.55 ± 49.53^{a}	100.01 ± 13.32^{a}	0.091
Toughness (MJ/m^3)	15.69 ± 3.30^{a}	10.03 ± 2.64^{a}	8.66 ± 5.21^{a}	9.69 ± 1.84^{a}	0.135

Significant differences between means for a given property are indicated by letters in superscripts; means sharing at least one letter are not significantly different ($P_{\mathrm{Tukey}} \geq 0.05$)

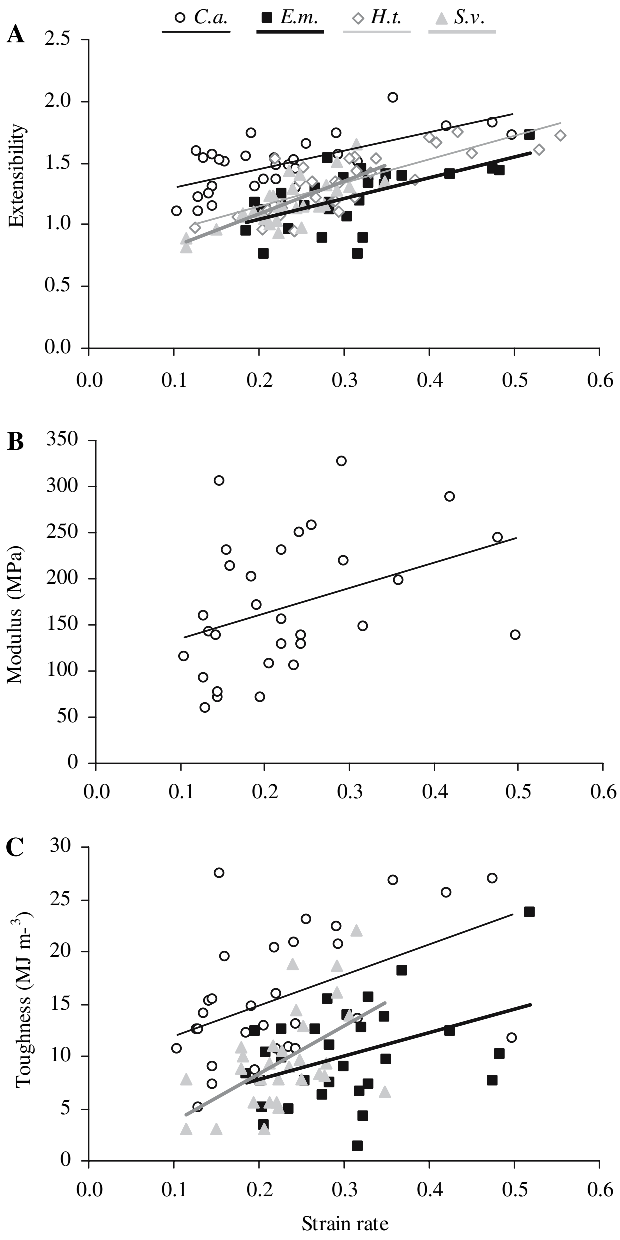

Fig. 3 *Colobocentrotus atratus*, *Echinometra mathaei*, *Heterocentrotus trigonarius* and *Stomopneustes variolaris*. Relationships between tube foot stem mechanical properties (i.e., **a** extensibility, **b** modulus, and **c** breaking energy density) and strain rate. Only the properties and species for which the slopes of the linear regressions were significantly different from zero were plotted (linear regressions, $P_{\text{test}} < 0.05$)

(Table 3). Microscopic observation of the adhesive footprints left on the substratum after tube foot detachment showed that not all footprints were complete, i.e., circular and evenly stained. Incomplete footprints were presumably left by tube feet that had adhered with only a fraction of their disc surface (see also Santos and Flammang 2006). Two footprint surface areas were, therefore, measured: the stained surface area and the maximum surface area calculated from the diameter of circular footprints (Table 3). The former was used to calculate the disc tenacity and the latter to calculate the disc maximum attachment force (Table 3). These two adhesion parameters were significantly higher in *C. atratus* than in the three sympatric species (Table 3; Fig. 4)

Individual sea urchin morphometry and attachment strength

Table 4 summarizes the morphometric and tenacity measurements of individual sea urchins from the four species studied. In terms of test dimensions, there were significant differences among the four species (Fig. 1i–p). *Heterocentrotus trigonarius* and *Stomopneutes variolaris* had the largest tests, followed by *C. atratus* and finally by *E. mathaei*. *H. trigonarius* had also the highest test, followed by *S. variolaris*, *E. mathaei* and *C. atratus*. *H. trigonarius* had the highest test height/diameter ratio (H:D = 0.66) indicating that this species had the roundest test, followed by *E. mathaei* (H:D = 0.60), *S. variolaris* (H:D = 0.54) and finally by *C. atratus* which had the lowest H:D ratio (0.40) and thus the flattest test. However, when spines were taken into consideration, the three species with a more typical echinoid morphology presented a lower H:D ratio (0.36, 0.46 and 0.48 for *H. trigonarius*, *S. variolaris* and *E. mathaei*, respectively) than *C. atratus* (0.61) (Fig. 1a–h).

Colobocentrotus atratus was the species, which had the highest number of adoral tube feet ($\approx$770), approximately twice as numerous as those of *H. trigonarius* and *S. variolaris* ($\approx$400) and almost four times in comparison with *E. mathaei* ($\approx$215) (Table 4; Fig. 5b). In all four species, a significant positive linear relationship ($r^2 > 0.99$, $P < 0.04$) existed between the number of adoral tube feet (TF) and the diameter of the test (TD, expressed in mm). Therefore, the following equations were used to estimate the number of adoral tube feet of the 30 sea urchins of each species used in the experiments:

$$\textit{Colobocentrotus atratus}\ \mathrm{TF} = 41.16\ \mathrm{TD} - 665.64 \tag{7}$$

$$\textit{Echinometra mathaei}\ \mathrm{TF} = 9.07\ \mathrm{TD} - 54.23 \tag{8}$$

$$\textit{Heterocentrotus trigonarius}\ \mathrm{TF} = 5.71\ \mathrm{TD} + 162.23 \tag{9}$$

$$\textit{Stomopneustes variolaris}\ \mathrm{TF} = 8.15\ \mathrm{TD} + 71.9 \tag{10}$$

.

Individual sea urchin tenacity was always size- and weight-independent ($P > 0.05$ for linear regressions of tenacity against test diameter, height and weight), thus allowing interspecific comparisons. Furthermore, no significant intraspecific difference was found in the attachment force, adhesive surface area or tenacity

Table 3 Mean (±SD) morphometric and tenacity values of single tube foot of *Colobocentrotus atratus, Echinometra mathei, Heterocentrotus trigonarius* and *Stomopneustes variolaris*

	Species				P_{ANOVA}
	Colobocentrotus atratus	*Echinometra mathaei*	*Heterocentrotus trigonarius*	*Stomopneutes variolaris*	
Number of individuals	7	7	6	4	
Attachment force (N)	0.28 ± 0.12^{b}	0.06 ± 0.03^{a}	0.12 ± 0.02^{a}	0.11 ± 0.07^{a}	0.001
Adhesive surface area (mm^2)					
Circular footprints	0.81 ± 0.27^{ab}	0.46 ± 0.20^{a}	1.03 ± 0.16^{b}	0.92 ± 0.34^{b}	0.001
Stained footprints	0.51 ± 0.19^{a}	0.35 ± 0.17^{a}	0.64 ± 0.25^{a}	0.54 ± 0.21^{a}	0.150
Tenacity (MPa)	0.54 ± 0.18^{b}	0.22 ± 0.10^{a}	0.25 ± 0.16^{a}	0.21 ± 0.09^{a}	0.001
Estimated maximum attachment force (N) *	0.47 ± 0.16^{b}	0.11 ± 0.05^{a}	0.26 ± 0.17^{a}	0.20 ± 0.09^{a}	0.001

Significant differences between means for a given parameter are indicated by letters in superscripts; means sharing at least one letter are not significantly different ($P_{\text{Tukey}} \geq 0.05$)

* Calculated as the product of the surface area of circular footprints by the tenacity

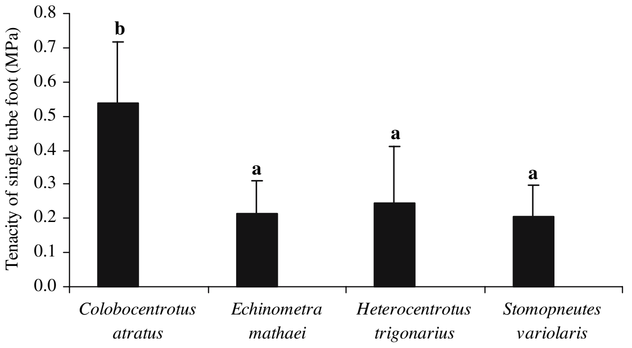

Fig. 4 *Colobocentrotus atratus*, *Echinometra mathaei, Heterocentrotus trigonarius* and *Stomopneustes variolaris*. Mean values (±SD, $n > 4$) of tenacity measured on single tube foot attached to a polymethylmethacrylate substratum

obtained with the three angles of traction (0°, 45° and 90°) ($P_{\text{ANOVA}} > 0.05$). Therefore, data were pooled within each species.

The interspecific analysis, did not detect any significant difference in tenacity (Table 4; Fig. 5a) although both the detachment forces and the adhesive surface areas differed significantly among species. As for the number of adoral tube feet involved in attachment it varied significantly among the four species ($P_{\text{ANOVA}} = 0.001$), *S. variolaris* employing more tube feet to attach than the other three species (Fig. 5b). Detachment force was always positively correlated with the adhesive surface area ($P \leq 0.001$, $r \geq 0.67$) and with the number of attached tube feet ($P \leq 0.001$, $r \geq 0.68$).

Common to the four species, was the occasional failure of the stem prior to the detachment of the disc. Although, the number of broken tube feet was lower in *E. mathaei* (Fig. 5b), in terms of percentage no significant interspecific difference was found ($P_{\text{ANOVA}} = 0.42$). Moreover, the number of broken tube feet was found to be positively correlated with both the detachment force in the four species ($P \leq 0.004$, $r \geq 0.51$), and with the number of attached tube feet in all the species but *S. variolaris* ($P \leq 0.006$, $r \geq 0.49$).

Safety factor

The maximum hydrodynamic force exerted on sea urchins is directly proportional to their projected profile (S_{profile}) and planform (S_{planform}) surface areas exposed, respectively, to lift and drag forces. *H. trigonarius* was the species with the largest projected surface areas followed, in decreasing order, by *S. variolaris*, *E. mathaei* and *C. atratus* (Table 4). However, based on three representative individuals per species, the ranges of these measured surface areas overlap between the different species. Values for the coefficients of drag and lift for *C. atratus* and *E. mathaei* are those reported by Denny and Gaylord (1996); for the two other species used in this study, the coefficients were assumed to be similar to those reported for *E. mathaei*, based on similar morphology. A good estimate of the maximum attachment force of an individual sea urchin can be obtained when tenacity is multiplied by the maximum adhesive surface area (Santos and Flammang 2007). The latter takes into account the total number of adoral tube feet and the adhesive surface of a single tube foot footprint (circular footprint). In this way, the maximum attachment forces are 148, 26, 82 and 76 N for *C. atratus*, *E. mathaei*, *H. trigonarius* and *S. variolaris*, respectively, when estimated from whole individual tenacity; and 336, 21, 100 and 76 N when estimated from single tube foot tenacity. Figure 6 shows the evolution of the safety factor in function of the water velocity. When this factor is calculated using the maximum attachment forces estimated from

Table 4 Mean values (±SD, $n = 30$ except when indicated) morphometric and tenacity values of individual sea urchins from the species *Colobocentrotus atratus*, *Echinometra mathei*, *Heterocentrotus trigonarius* and *Stomopneustes variolaris*

	n	Species				P_{ANOVA}
		Colobocentrotus atratus	*Echinometra mathaei*	*Heterocentrotus trigonarius*	*Stomopneutes variolaris*	
A. Morphometric measurements						
Test diameter (mm)	30	34.8 ± 5.4^{b}	29.6 ± 3.8^{a}	40.8 ± 7.9^{c}	40.4 ± 8.7^{c}	0.001
Test height (mm)	30	14.0 ± 1.9^{a}	18.0 ± 3.1^{b}	27.1 ± 6.3^{d}	21.6 ± 6.0^{c}	0.001
Total length including spines (mm)*	3	51.0–59.1 (54.5)	60.6–72.9 (65.6)	77.6–134.5 (113.3)	74.8–119.2 (96.4)	
Profile surface area (mm^2)*	3	1,065–1,411 (1182.9)	1,139–1,695 (1,467.4)	1,447–3,313 (2,483.9)	788–2,428 (1,512.8)	
Planform surface area (mm^2)*	3	1,299–1,845 (1,524.2)	1,656–2,322 (1,898.1)	1,982–5,869 (4,184.9)	1,388–4,600 (3,029.0)	
Immersed weight (g)	30	5.33 ± 2.58^{a}	4.60 ± 1.68^{a}	23.87 ± 10.57^{c}	10.45 ± 5.57^{b}	0.001
Number of adoral tube feet	30	766 ± 222^{c}	214 ± 34^{a}	396 ± 45^{b}	401 ± 71^{b}	0.001
B. Tenacity measurements	30					
Attachment force (N)		16.88 ± 11.44^{b}	2.96 ± 2.83^{a}	14.62 ± 8.94^{b}	25.01 ± 13.53^{c}	0.001
Adhesive surface area (mm^2)		82.63 ± 52.30^{b}	12.82 ± 10.31^{a}	91.86 ± 83.09^{b}	175.68 ± 155.80^{c}	0.001
Tenacity (MPa)		0.24 ± 0.16^{a}	0.26 ± 0.15^{a}	0.20 ± 0.09^{a}	0.21 ± 0.12^{a}	0.246

Significant differences between means for a given parameter are indicated by letters in superscripts; means sharing at least one letter are not significantly different ($P_{\text{Tukey}} \geq 0.05$)

* Minimum–maximum (and mean) values for three individuals whose sizes covered the range of sizes of the animals collected in the sampling area

individual sea urchin tenacity (solid lines in Fig. 6), it predicts that individuals of *E. mathaei* would be the first to be dislodged, at water velocities of 7.5 m s^{-1}, followed by individuals of *S. variolaris*, *H. trigonarius* and *C. atratus* at water velocities of 10, 12.5 and 17.5 m s^{-1}, respectively. When the safety factor was calculated using the maximum attachment forces estimated from single tube foot tenacity (dashed lines in Fig. 6), dislodgement velocities remains similar except in *C. atratus* which could resist particularly high water speeds up to 27.5 m s^{-1}.

Discussion and conclusions

Single tube foot morphology and mechanical properties

Stem morphology is very similar in the four species investigated. Only the tube feet of *H. trigonarius* differed from those of the other species in having a thicker connective tissue layer. In terms of mechanical properties, the stems of *C. atratus* presented the highest mean values of extensibility, strength, stiffness and toughness (1.49, 60, 170 MPa and 15.7 MJ/m^3, respectively). Nevertheless, among these parameters only stem extensibility was found to be significantly superior, and only relatively to the values obtained with *S. variolaris* tube feet. These results can be compared with those reported by Santos and Flammang (2005) for the tube feet of three European sea urchins, *Arbacia lixula* (Linné, 1758), *Paracentrotus lividus* (Lamark, 1816) and *Sphaerechinus granularis* (Lamark, 1816). As in the present study, the tube feet morphometry of these three European species was quite similar. When compared with tropical species, the tube feet of European echinoids presented similar stem diameters but relatively thinner stem walls, representing 20% of the stem diameter (i.e., 10% less than in tropical species). The thickness and cross-sectional areas of the various stem tissue layers were consequently more important in the tropical species than the European ones, but when expressed as a percentage of the stem wall the values were identical. The stem mechanical properties were also higher in the tube feet of tropical sea urchin, except for stem stiffness, which was lower in the tropical echinoids but partially overlapping the values, measured in European species (152–328 MPa; Santos and Flammang 2005).

In the four studied species, stem extensibility was positively dependent on strain rate (40–60% of variation explained); and, with the exception of *H. trigonarius*, stem toughness was also significantly influenced by the variation in strain rate (17–28% of variation explained). These results indicate that sea urchins tube feet become more extensible and require more energy to be extended and broken with increasing strain rate. A similar dependence (as well as for the other stem mechanical properties) was

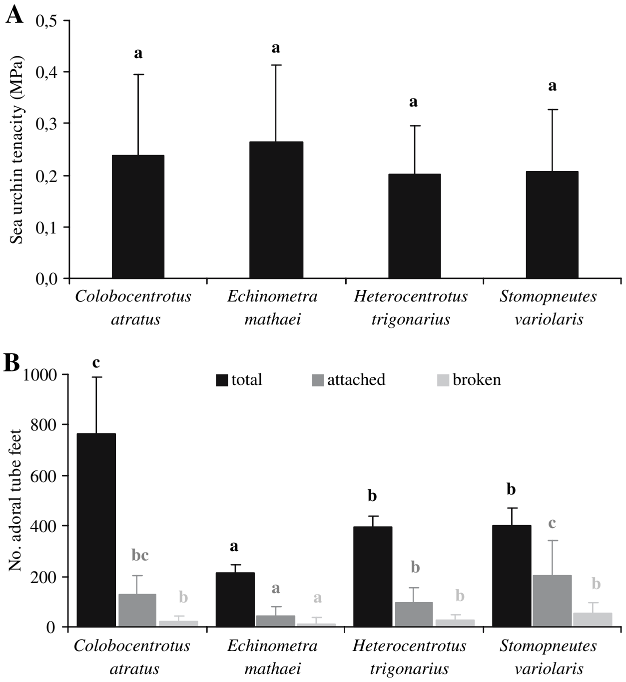

Fig. 5 *Colobocentrotus atratus*, *Echinometra mathaei, Heterocentrotus trigonarius* and *Stomopneustes variolaris*. **a** Mean values (±SD, $n = 30$) of tenacity measured for individual sea urchins attached to a polystyrene substratum. **b** Mean number of total (*black bars*), attached (*dark grey bars*) and broken (*bright grey bars*) adoral tube feet. Significant interspecific differences between means are indicated by *letters* in superscript; means sharing at least one letter are not significantly different ($P > 0.05$, multiple comparison test of Tukey)

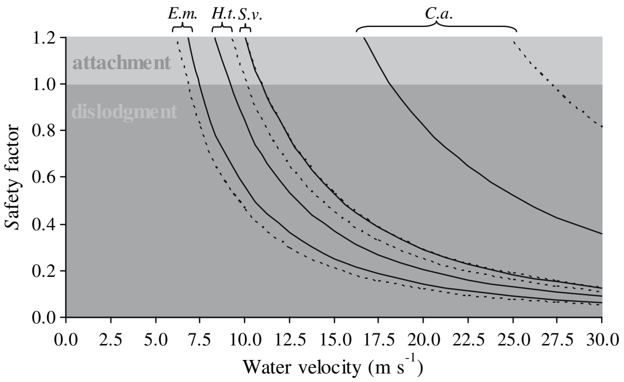

Fig. 6 *Colobocentrotus atratus*, *Echinometra mathaei, Heterocentrotus trigonarius* and *Stomopneustes variolaris*. Variation of the safety factor as a function of water velocity. Factor calculated with the maximum attachment forces estimated from the mean tenacities measured for individual sea urchin (*solid lines*) and single tube foot (*dashed lines*). *Light* and *dark grey* areas indicate factor values corresponding to sea urchin attachment or dislodgement, respectively

reported for relaxed tube feet of *Strongylocentrotus droebachiensis* (O.F. Müller, 1776) and of *P. lividus* (Leddy and Johnson 2000; Santos and Flammang 2005, respectively). Therefore, in the natural environment, most stem mechanical properties are increased when tube feet are subjected to rapid loads (such as waves) compared to slower loads (such as self-imposed protraction). The resultant increase in the amount of energy needed to break the tube feet thus provides an adaptative advantage to the sea urchin.

Morphologically, the tube foot discs of *C. atratus* and *S. variolaris* had an intermediate adhesive surface area (about 0.8 mm^2), larger than the one of the discs of *E. mathaei* (0.5 mm^2) but smaller than the one of the discs of *H. trigonarius* (1 mm^2). The measurements of disc tenacity revealed that *C. atratus* tube feet could attach with a tenacity (0.54 MPa) twice higher than that of *E. mathaei*, *H. trigonarius* and *S. variolaris* (0.21–0.25 MPa). These values are in the same range as those reported with single tube foot from the sea urchin *P lividus* when attached to PMMA (0.34 MPa), PS (0.29 MPa) and glass (0.30 MPa) substrata (Santos and Flammang 2006).

It has been often suggested that the degree of development of sea urchins tube feet is intimately related with the maximum environmental energy a species can withstand (Sharp and Gray 1962; Smith 1978). Based on this assumption, Smith (1978) categorized regular echinoid coronal tube feet in four types based on their morphologies. Type 1 tube feet do not possess a terminal disc, their apex consisting of a small sensory pad without any skeletal framework, and their stem possesses thin connective tissue layer and retractor muscle. Conversely, type four tube feet bear a large, well-developed disc and their stem possesses thick connective tissue and muscle layers. Types two and three tube feet are intermediates between the structures of types one and four tube feet. Furthermore, this morphological gradation is thought to be associated with an increasing adhesive power of the disc (Smith 1978; Flammang 1996) and an increasing strength of the stem (Leddy and Johnson 2000). Therefore, sea urchin species possessing type two tube feet were described as being restricted to soft or firm sediment bottoms in low to moderate energy environments while those possessing type four tube feet as inhabiting steep rocky bottoms or coral reefs in high energy environments (Smith 1978). Type three tube feet would be found in species living on rocks in intermediate environments, being restricted to burrows or crevices when exposed in high-energy environments. According to Smith (1978), *C. atratus* possesses type four tube feet, *E. mathaei* and *S. variolaris* have type three tube feet and *H. trigonarius* has tube feet in-between types three and four. However, our morphological results do not support Smith's (1978) classification. Indeed, the most developed tube feet were those of *H. trigonararius* (both in terms of stem wall thickness and disc adhesive surface area), but this does not translate into better mechanical properties. Inversely, the best tube feet in terms of mechanical properties were those of *C. atratus*, which were intermediate in terms of morphometrics. A similar conclusion was reached by Santos and Flammang (2005, 2006) for the tube feet of European species.

There seems to be enough evidence that a species habitat cannot be related to the degree of development of its tube feet as postulated by Smith (1978). However, a relationship between the level of hydrodynamic exposure and the mechanical properties of tube foot stem and disc can be pointed out. In the study site described by Santos and Flammang (2005, 2006), *P. lividus* was the most exposed of the three species and its tube feet showed the highest disc tenacity and stem stiffness. Similarly, the most exposed species at Cap La Houssaye, *C. atratus*, have tube feet with the highest disc tenacity and stem extensibility. It is noteworthy that values for some of the mechanical properties of the tube feet of *C. atratus* are also the highest reported so far for any echinoderm tube foot, comparing to barnacle cement in terms of tenacity and to mussel byssus in terms of material toughness (see Yule and Walker 1987; Bell and Gosline 1996, respectively). Nevertheless, other factors such as tube foot number and arrangement, and sea urchin size and shape must also be taken into account in order to fully understand species resistance to hydrodynamic exposure.

Individual sea urchins morphometrics, tenacity and safety factor

Of the four species studied, *H. trigonarius* and *S. variolaris* had the biggest tests followed by *E. mathaei* and *C. atratus*. In terms of test shape, *H. trigonarius* had the roundest test and *C. atratus* the flattest one, while the other two species presented intermediate shapes. Curiously, the species possessing the highest number of adoral tube feet were not the biggest ones. Indeed, *C. atratus* had approximately twice as many adoral tube feet to attach, as *H. trigonarius* and *S. variolaris*, and almost four times in comparison with *E. mathaei*. These results together with the observed strong positive relationship between the detachment force and the number of attached tube feet confirm Märkel and Titschack (1965) supposition that species ability to resist higher detachment forces is related with a greater number of adoral tube feet involved in attachment. This increased number of tube feet can be attributed to the presence of enlarged ambulacral areas in the adoral portion of the test, the so-called called phyllodes (Kier 1974; Lawrence 1987). Phyllodes are strongly developed in echinoids exposed to heavy surf such as *Colobocentrotus* and *Heterocentrotus* (Kier 1974). In *C. atratus*, these phyllodes often possessed five rows of closely gathered tube feet, while in *H. trigonarius* they contained four rows of more dispersed tube feet (Fig. 1m, o; Kier 1974). The function of phyllodes is to increase the number of tube feet, primarily for attachment to the substratum but also to counteract the stress imposed by the movement of the teeth in grasping food off the substratum (Kier 1974). As for *S. variolaris* and *E. mathaei* they do not possess phyllodes and their ambulacral areas have, respectively, three and two rows of tube feet.

In our laboratory conditions, detachment force was positively correlated with the number of broken tube feet, indicating that the overall attachment strength may be limited by the number of stems which fail before disc detachment, as previously suggested by Märkel and Titschack (1965). The mean percentages of broken tube feet compared to detached tube feet were 19, 25, 26 and 31% for *C. atratus*, *E. mathaei*, *H. trigonarius* and *S. variolaris*, respectively. It may seem strange that a significant number of tube feet tear as the mean breaking force of the stem is always superior to the estimated maximum attachment force of the disc (compare Tables 2 and 3). However, by simply comparing this maximum attachment force of the disc to the distribution of stem breaking forces, 4–24% of the tube feet are predicted to break, according to the species considered. Variability of stem tensile strength thus explains, at least partly, the observed proportions. The positive strain rate dependence of stem mechanical properties also suggests that, at the very high strain rates applied by waves ($\gg 1\ \mathrm{s}^{-1}$;Denny 1988), the performance of tube foot stems may be improved and failure percentages reduced.

Contrary to single tube foot tenacity, whole sea urchin tenacity did not show any significant interspecific difference. In fact, in *E. mathaei*, *H. trigonarius* and *S. variolaris* the tenacity of individual sea urchins was approximately the same as the tenacity of single tube foot, but in *C. atratus* the former was about half the latter. Although the explanation for this difference is unclear, a possibility could be that the two measurements were done on different substrata, PMMA for single tube feet and PS for individual sea urchins. It is known that substratum preference (the ability to develop a higher tenacity on one substratum compared to another one) varies from species to species (Sharp and Gray 1962; Santos and Flammang 2007).

Estimated maximum attachment force for *C. atratus* averages 148 N when calculated with individual sea urchin tenacity, and 336 N when calculated with single tube foot tenacity. On the other hand, attachment forces measured in situ for the same species range from 60 to 250 N (Gallien 1987). These high attachment forces have the important consequence of enabling this species to resist high dislodgement forces and thus venture onto rock surfaces fully exposed to wave-induced velocities and accelerations. This has been confirmed by calculating a safety factor integrating water velocity with sea urchin size, shape and hydrodynamic coefficients. This safety factor compares the hydrodynamic force experienced by an organism with the maximum attachment force it can produce to resist water movements. Accelerations forces were not accounted for in the present study because, although rapid accelerations are common on wave-swept shores, the spatial scale of acceleration is quite small and so even if a large sea urchin displaces a substantial volume of water, acceleration will not be coherent over the entire animal, and the accelerational force will still be much smaller than drag and lift (Gaylord 2000). From the variation of safety factor with water velocity, it was observed that *C. atratus* strong attachment force allows it to resist dislodgment up to water velocities of 17.5 m s^{-1} and even close to 27.5 m s^{-1} if single tube foot tenacity is used in the calculation. The latter velocity is about the highest ever recorded in the wave-swept environment (Denny et al. 2003). In contrast, the more typical echinoid *E. mathaei* is predicted to be dislodged by water velocities superior to 7.5 m s^{-1}. If the safety factor were recalculated assuming that *C. atratus* had the same attachment force of *E. mathei*, or vice-versa, both species would be predicted to be dislodged at the same water velocities. Thus, this seems to indicate that the differences in drag and lift coefficients resulting from the different shape of both species are of little importance relative to their attachment force. However, in *C. atratus*, the morphological trade off between drag and lift (reduction in drag offset by an increase in lift; Denny and Gaylord 1996) may have a positive hydrodynamic consequence. Indeed, although it does not change the overall environmental force placed on the animal, it increases the ratio of normal force (perpendicular to the substratum) to shear force (parallel to the substratum), thus spreading the load more evenly on all tube feet.

Size also matters for the calculation of the safety factor. This is why the large *H. trigonarius* is dislodged at approximately the same water velocity as the smaller *E. mathaei* even though its maximal adhesion force is four times higher (assuming that using the same hydrodynamic coefficients for both species is valid). A comparative study with three species from the Mediterranean Sea also demonstrated that the largest species investigated, *S. granularis*, despite having the highest attachment force and highest number of adoral tube feet, would be dislodged at lower water speeds than the smaller *A. lixula* and *P. lividus* (Santos and Flammang 2007).

In view of the present results, *C. atratus* ability to inhabit areas of extreme water velocities seems to be intimately related with its very high number of adoral tube feet and not to its peculiar morphology. In this respect, the shingle sea urchin is similar to limpets, in which shell shape is independent of the risk of dislodgement by waves but respond to other selective factors (Denny 2000). However, the streamlined morphology of *C. atratus* might be an adaptation to obviate other hydrodynamic stresses such as wave impact. Indeed, Gaylord (2000) demonstrated that sharp, transient forces arising from the impingement of waves directly on non-submerged rigid organisms may impose the most severe loadings experienced by animals in the intertidal. The high location of *C. atratus* on the shore exposes individuals of this species to such impact-type forces. In this context, having modified aboral spines can also reduce the risk of spine breakage or damage, which is common in species from exposed habitats, and in turn reduces the energetic costs associated with spine repair (Régis and Thomassin 1982; Gallien 1987; Rogers-Bennett et al. 1995). Finally, other selective environmental pressures should not be discarded and are worth further research. For instance, *C. atratus* morphology seems also well suited for the retention of extra corporeal water, which can be essential to resist the thermal and desiccation stresses during low tides (Gallien 1987; Denny and Gaylord 1996).

Acknowledgments The authors thank the Director and staff of ECOMAR—Laboratoire d'Ecologie Marine (Saint Denis, Reunion Island), especially Prof. C. Conand, and of the "Aquarium de la Réunion" (Saint Gilles les Bains, Réunion Island) for sea urchin maintenance. Thanks also to Dr. D. Lanterbecq for valuable help in field and experimental work, and to P. Postiau for technical assistance. Work supported in part by a FRFC Grant no. 2.4532.07. R. S. is benefited from a doctoral grant of the Foundation for Science and Technology of Portugal (SFRH/BD/4832/2001). P.F. is a Senior Research Associate of the Fund for Scientific Research of Belgium (F.R.S.–FNRS). This study is a contribution from the Centre Interuniversitaire de Biologie Marine (CIBIM; http://www.ulb.ac.be/sciences/biomar/).

References

Agassiz A (1908) The genus *Colobocentrotus*. Mem Mus Comp Zool 39:1–33

Bell EC, Gosline JM (1996) Mechanical design of mussel byssus: material yield enhances attachment strength. J Exp Biol 199:1005–1017

Conand C, Chabanet P, Gravier-Bonnet N (2003) Biodiversité du milieu récifal réunionnais: échinodermes, poissons et hydraires. Rapport au Conseil Régional

De Ridder C (1986) Les Echinides. In: Guille A, Laboute P, Menou JL (eds) Guide des étoiles de mer, oursins et autres échinodermes du lagon de Nouvelle-Calédonie. Editions de l'ORSTOM, Paris, pp 23–53

Denny MW (1988) Biology and mechanics of the wave-swept environment. Princeton University Press, Princeton

Denny M (2000) Limits to optimization: fluid dynamics, adhesive strength and the evolution of shape in limpet shells. J Exp Biol 203:2603–2622

Denny M, Gaylord B (1996) Why the urchin lost its spines: hydrodynamic forces and survivorship in three echinoids. J Exp Biol 199:717–729

Denny M, Miller L, Stokes M, Hunt L, Helmuth B (2003) Extreme water velocities: Topographical amplification of wave-induced flow in the surf zone of rocky shores. Limnol Oceanogr 48:1–8

Ebert TA (1982) Longevity, life history, and relative body wall size in sea urchins. Ecol Monogr 52:353–394

Flammang P (1996) Adhesion in echinoderms. In: Jangoux M, Lawrence JM (eds) Echinoderm studies, vol 5. Balkema, Rotterdam, pp 1–60

Gallien B (1987) A comparison of hydrodynamic forces on two sympatric sea urchins: implications of morphology and habitat. MSc thesis. University of Hawaii, Honolulu

Gaylord B (2000) Biological implications of surf-zone flow complexity. Limnol Oceanogr 45:174–188

Hyman LH (1955) The invertebrates: Echinodermata. McGraw-Hill, New York

Lawrence J (1987) A functional biology of echinoderms. Croom Helm, London

Leddy HA, Johnson AS (2000) Walking versus breathing: mechanical differentiation of sea urchin podia corresponds to functional specialization. Biol Bull 198:88–93

Kier PM (1974) Evolutionary trends and their functional significance in the post-paleozoic echinoids. J Paleontol 48:1–95

Märkel K, Titschack H (1965). Das Festhaltevermögen von Seeigeln und die Reißfestigkeitihrer Ambulacralfüßchen. Sond Zeit Naturw 10:268

Mortensen T (1943) A monograph of the Echinoidea–Camarodonta. CA Reitzel, Copenhagen

Régis MB, Thomassin BA (1982) Ecologie des échinoïdes réguliers dans les récifs coralliens de la région de Tuléar (S.W. de Madagascar): adaptation de la microstructure des piquants. Ann Inst Océanogr 58:117–158

Rogers-Bennett L, Bennett WA, Fastenau HC, Dewees CM (1995) Spatial variation in red sea urchin reproduction and morphology: implications for harvest refugia. Ecol Appl 5:1171–1180

Santos R, Flammang P (2005) Morphometry and mechanical design of tube foot stems in sea urchins: a comparative study. J Exp Mar Biol Ecol 315:211–223

Santos R, Flammang P (2006) Morphology and tenacity of the tube foot disc of three common European sea urchin species: a comparative study. Biofouling 22:187–200

Santos R, Flammang P (2007) Intra- and interspecific variation of attachment strength in sea urchins. Mar Ecol Prog Ser 332:129–142

Santos R, Gorb S, Jamar V, Flammang P (2005) Adhesion of echinoderm tube feet to rough surfaces. J Exp Biol 208:2555–2567

Shadwick RE (1992) Biomechanics–Materials, A Practical Approach. Oxford University Press, Oxford

Sharp DT, Gray IE (1962) Studies on factors affecting local distribution of two sea urchins, *Arbacia punctulata* and *Lytechinus variegatus*. Ecology 43:309–313

Smith AB (1978) A functional classification of the coronal pores of echinoids. Paleontology 21:759–789

Vogel S (2003) Comparative biomechanics—life's physical world. Princeton University Press, Princeton

Yule AB, Walker G (1987) Adhesion in barnacles. In: Southward AJ (ed) Crustacean Issues, vol 5, biology of barnacles. Balkema, Rotterdam, pp 389–402